Proceedings of BALTTRIB'2026 edited by prof. J. Padgurskas
eISSN 2424-5089 (Online) DOI: 10.15544/balttrib.2026.1

CRITERIA FOR EVALUATING PROCESSES IN THE FRICTIONAL CONTACT ZONE OF COMPOSITE MATERIALS

A. Gypka[1], O. Liashuk, O. Tson, D. Mironov, R. Khoroshun, V. Teslia
Ternopil Ivan Puluj National Technical University, Ukraine

Abstract: This study investigates approaches to improving the wear resistance of heavily loaded tribological interfaces in automotive components using composite materials with enhanced tribological properties. The research is based on the principles of structural and energy adaptation of materials to friction and wear conditions. The tribological characteristics of Cu–Pb alloys, an Fe–Cu composite, and a zirconia-based composite material were evaluated experimentally. The dependence of the coefficient of friction, specific work of surface degradation, and energy capacity of the tribosystem on specific contact load was determined at a constant sliding speed, and the structural adaptation of the investigated materials during contact interaction was analyzed. Experimental tests were conducted using a universal tribometer in a pin-on-disc configuration with pure petroleum jelly as the lubricant. The experimental results were analyzed using a systems approach and the developed set of parameters for characterizing tribological interfaces.

Keywords: composite materials; coefficient of friction; specific contact load; structural and energy adaptation; specific work of surface degradation; energy capacity of the tribosystem; tribometer.

1. INTRODUCTION

The investigation of heavily loaded tribological interfaces in automotive components is an important task in modern automotive engineering [1–3]. Friction and wear processes occurring in the contact zone between working surfaces determine the reliability and service life of components and assemblies [4]. Therefore, the use of materials capable of maintaining stable friction characteristics and enhanced wear resistance under high contact loads isof considerable practical importance [5, 6].

The tribological behaviour of materials is governed by the interaction of mechanical, kinetic, energy, and thermal factors within the tribosystem [7–9]. During structural and energy adaptation, protective dissipative secondary structures (DSS) form on the friction surfaces, contributing to the stabilisation of tribological parameters and a reduction in wear intensity [10]. Their formation depends on material properties, specific contact load, sliding speed, and lubrication conditions [11,12]. Accordingly, the assessment of structural and energy adaptation requires a comprehensive analysis of friction and wear characteristics and energy parameters, considering the contact interaction conditions [13].

This study investigates Cu–Pb alloys, a sintered Fe–Cu composite material, and ZrO_2–5.3% Y_2O_3 ceramic. Their tribological behaviour was compared using the coefficient of friction, specific work of surface degradation, and the thermal indicator of the energy capacity of the tribosystem. Fe–Cu was selected from the investigated materials for microscopic examination. Micrographs of its friction surface were used to analyse differences in surface morphology between the stable friction regime and the surface damage regime [14].

2. EXPERIMENTAL

The research methodology involved comparative tribological testing of materials with identical contact geometry, constant sliding speed, and unchanged lubrication conditions, while the specific contact load was increased stepwise. Friction and wear processes were assessed by combining the recording of tribological parameters, the calculation of energy indicators, and microscopic

[1] Author for contacts: Assis. Prof. dr. Andrii Gypka
E–mail: Gypkab@gmail.com

Copyright © 2024 The Authors. Published by Vytautas Magnus University, Lithuania. This is an open-access article distributed under the terms of the Creative Commons Attribution License (CC-BY 4.0), which permits unrestricted use, distribution, and reproduction in any medium, provided the original author and source are credited.

examination of the friction surfaces. The following subsections describe the materials and specimens, test conditions and procedure, surface examination methods, and evaluation criteria.

2.1. Materials, test conditions, and surface examination

The investigated materials comprised Cu–Pb alloys containing 70% Cu–30% Pb and 50% Cu–50% Pb, a sintered Fe–Cu composite containing 6% Cu, and ZrO_2–5.3% Y_2O_3 ceramic (Aidite 03HT). All specimens were cylindrical, with a diameter of 4 mm and a height of 11 mm. The counter body was a disc made of ShKh15 bearing steel, with a diameter of 120 mm, a thickness of 5 mm, a hardness of 55–62 HRC, and a working surface roughness of Ra = 0.63 μm.

The tests were conducted in a pin-on-disc configuration, with flat contact between the end face of the cylindrical specimen and the working face of the disc. To ensure comparability of the results, all specimens had the same contact geometry and an initial friction surface roughness of Ra = 0.32 μm. Lubrication conditions were identical for all investigated materials. Chemically inactive petroleum jelly was used as the lubricant and was supplied automatically to the friction zone to maintain continuous lubrication.

The sliding speed was maintained at V = 0.35 m/s. The specific contact load was increased stepwise through successive levels of 2, 4, 6, 8, 10, 12, and 14 MPa. Each load level was maintained for 10 h while the tribological parameters were recorded. Three replicate tests were performed for each material.

The morphology of the friction surfaces of the sintered Fe–Cu composite containing 6% Cu was examined using a Cam Scan 4DV scanning electron microscope. The micrographs were used to compare the surface condition in the stable friction regime and the surface damage regime.

2.2. Research methodology and evaluation criteria

The research methodology was based on a systems approach to evaluating friction and wear processes, taking into account the principles of structural and energy adaptation of materials in the frictional contact zone [2, 13]. The tribological interface was considered an open thermodynamic system whose state is governed by the properties of the contacting materials, specific contact load, sliding speed, lubrication conditions, and structural transformations in the surface layers. This approach was used to examine the relationships between the tribological and structural and energy parameters of friction and wear in the investigated materials.

To ensure comparability, all specimens were tested under identical contact conditions, with specific contact load P selected as the main controlled parameter. The response parameters were the coefficient of friction μ, the specific work of surface degradation A_p (Eq. 1), and the energy capacity of the tribosystem, expressed by the thermal indicator E_{CTQ} (Eq. 2). The specific work of surface degradation and the thermal energy capacity were calculated using the equations below, with the constituent quantities and their units defined accordingly.

$$A_p = \frac{A_f}{\Delta I} \tag{1}$$

Where: A_f – friction work, J; ΔI – wear intensity, mm^3.

$$E_{CTQ} = \frac{A_f}{\Delta T} \tag{2}$$

Where: A_f – friction work, J; ΔT – temperature change, K.

The tribological characteristics of the investigated materials were evaluated using a universal tribometer [15] (Fig. 1).



a) b)

Figure 1. General view of the tribometer friction pair (a) unit and loading mechanism (b)

The advantages of this tribometer include a wide range of smoothly adjustable loads, the capability for reversing the direction of motion, an open friction unit allowing visual observation of the tribological interface during operation, and specimen friction surfaces suitable for metallographic examination.

3. RESULTS AND DISCUSSION

3.1. Effect of specific contact load on friction characteristics and energy parameters

Figures 2–4 show the dependence of the coefficient of friction, specific work of surface degradation, and thermal energy indicator on specific contact load for the four materials described in Section 2.2..

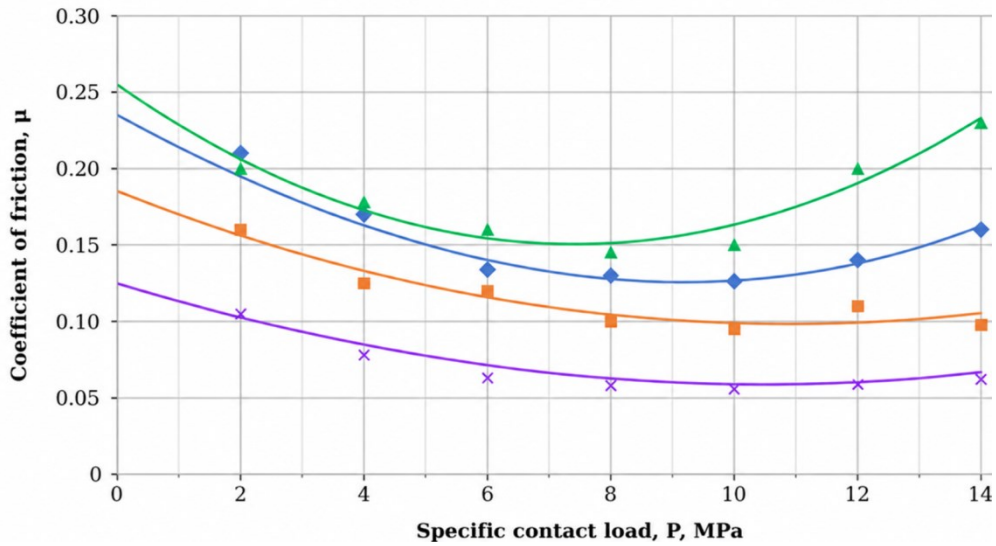

Figure 2. Variation of the μ with P: ♦ – alloy Cu–Pb (70% Cu + 30% Pb); ■ – sintered composite material Fe–Cu (6% Cu); ▲ – alloy Cu–Pb (50% Cu + 50% Pb); × – zirconium-based composite material (ZrO_2–5,3% Y_2O_3, Aidite 03HT)

The coefficient of friction exhibited a non-monotonic dependence on specific contact load (Fig. 2). The Cu–Pb 70/30 alloy showed relatively stable friction over the load range of 6–10 MPa, with μ remaining approximately between 0.12 and 0.14. For Cu–Pb 50/50, the range of relative stability was 5–10 MPa, with μ varying approximately between 0.15 and 0.16. At higher loads, the coefficient of friction of Cu–Pb 50/50 increased more markedly. Thus, increasing the Pb content did not reduce friction under the investigated conditions.

The Fe–Cu composite and ZrO_2–Y_2O_3 ceramic exhibited relatively stable friction over the load range of 8–14 MPa, with coefficients of friction of approximately 0.09–0.11 and 0.056–0.062, respectively. The ceramic maintained the lowest coefficient of friction throughout the investigated load range.

These results indicate that the tested materials differed both in the magnitude of the coefficient of friction and in the load range over which it remained relatively stable.

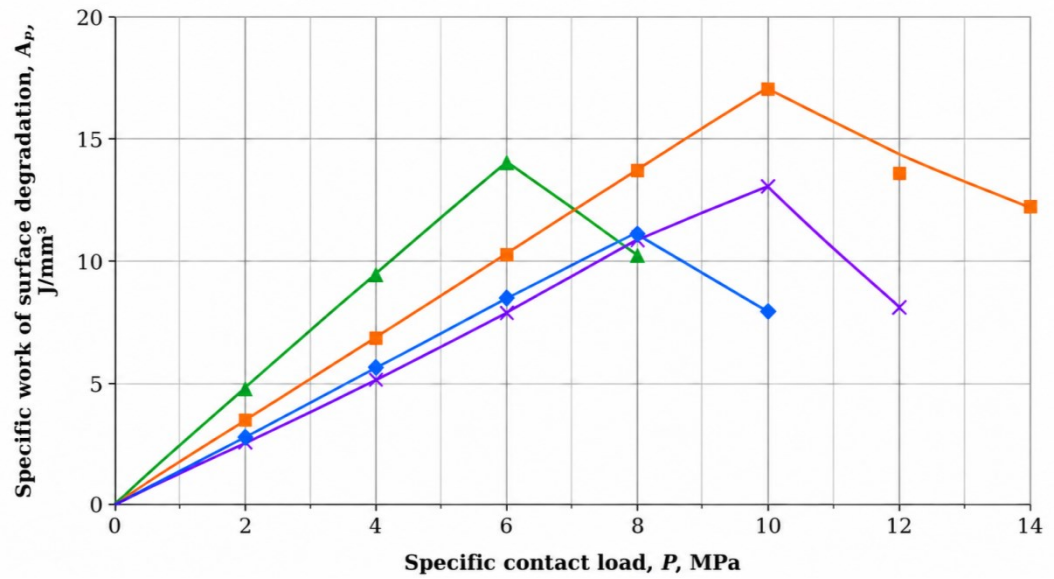

Figure 3. Variation of the A_P with P: ♦ – alloy Cu–Pb (70% Cu + 30% Pb); ■ – sintered composite material Fe–Cu (6% Cu); ▲ – alloy Cu–Pb (50% Cu + 50% Pb); × – zirconium-based composite material (ZrO_2–5,3% Y_2O_3, Aidite 03HT)

Analysis of the plotted relationships shows that the variation in the specific work of surface degradation A_p with specific contact load depended on the material (Fig. 3): the parameter increased to a maximum and then decreased. For the Cu–Pb 70/30 alloy, the maximum occurred at approximately 8 MPa. Cu–Pb 50/50 reached a higher maximum at approximately 6 MPa, with the subsequent decline beginning at a lower load.

The Fe–Cu composite exhibited the highest peak value of A_p, reached at approximately 10 MPa. The ZrO_2–Y_2O_3 ceramic reached its maximum at approximately 10 MPa. For all materials, A_p decreased markedly after reaching its respective maximum. Thus, the curves differed both in the magnitude of A_p and in the load at which its decline began.

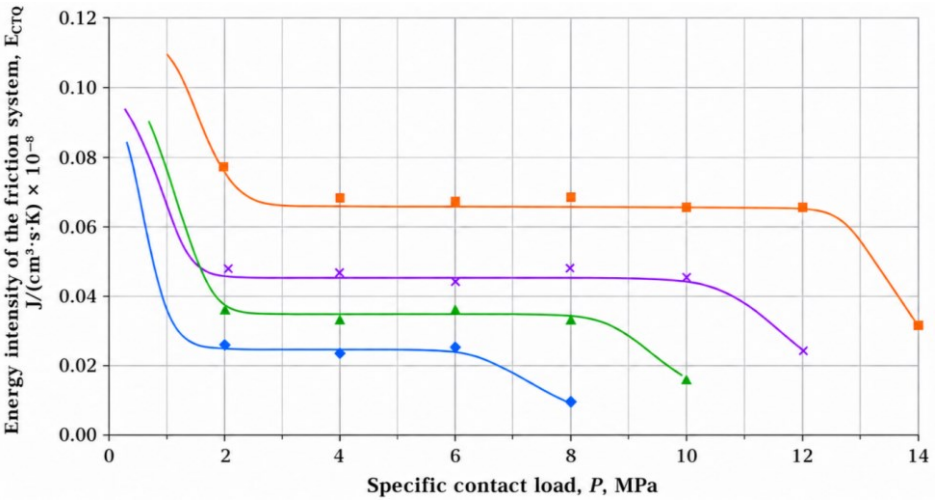

Figure 4. Variation of the E_{CTQ} with P: ♦ – alloy Cu–Pb (70% Cu + 30% Pb); ■ – sintered composite material Fe–Cu (6% Cu); ▲ – alloy Cu–Pb (50% Cu + 50% Pb); × – zirconium-based composite material (ZrO_2–5,3% Y_2O_3, Aidite 03HT)

As the specific contact load increased, E_{CTQ} exhibited three distinct regions (Fig. 4): an initial decrease, a region of relative stability, and a final decrease. For Cu–Pb 70/30, the parameter remained

at approximately 0.022 over the load range of 2–6 MPa. Cu–Pb 50/50 exhibited a higher stable level of approximately 0.035 over the range of 2–8 MPa, followed by a decrease.

The Fe–Cu composite exhibited the highest stable value of approximately 0.065 over the load range of 4–12 MPa. The ZrO_2–Y_2O_3 ceramic occupied an intermediate position, maintaining a value of approximately 0.045 over the range of 2–10 MPa. Thus, the curves differed both in the level of the thermal energy indicator and in the load range over which it remained relatively stable.

Thus, the three parameters characterise different aspects of the response to increasing contact load. Their combined assessment provides a more comprehensive comparison of the tested materials than the coefficient of friction alone.

3.2. Examination of the structural state of friction surfaces

The surface structure of the sintered Fe–Cu composite containing 6% Cu was examined to relate morphological signs of damage to changes in tribological and energy parameters. Figure 5 shows the surfaces after testing in the stable friction regime and during the transition to the surface damage regime.

In the normal friction and wear regime, characterised by minimum and stable values of μ and E_{CTQ} and a maximum value of A_p, the friction surface is covered by dissipative secondary structures (DSS) (Fig. 5a), as indicated by the relatively continuous surface regions.

During the transition to the surface damage regime, μ increases, whereas A_p and E_{CTQ} decrease. These changes are accompanied by changes in the surface structure (Fig. 5b).

Thus, the friction surface images complement the quantitative results by revealing differences in surface condition between the investigated regimes. Comparing these images with A_p and E_{CTQ} makes it possible to assess whether changes in the energy parameters are accompanied by visible damage to the surface layer.

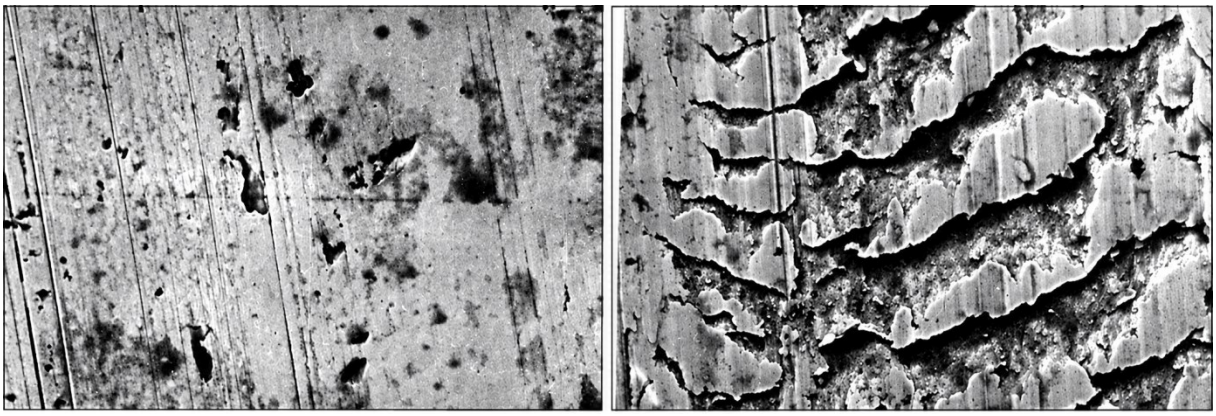

a) b)

Figure 5. Worn-surface morphology of the sintered Fe–Cu composite containing 6% Cu: (a) longitudinal grooves and localized depressions; (b) extensive surface discontinuities and regions of possible delamination.

The worn surface of one selected material was examined to characterize the morphological features formed during tribological testing. The micrographs presented below illustrate the surface condition and provide a basis for discussing possible wear mechanisms in relation to the friction and energy characteristics. This analysis is limited to the selected material and does not provide a comparison of surface morphology across all tested materials.

The surface structure was examined for all investigated materials within their respective ranges of stable friction and wear. Representative micrographs of Fe–Cu are presented in this study, as this material most clearly illustrated the differences between the trends in the coefficient of friction and the energy parameters.

4. CONCLUSIONS

The investigated materials exhibited different changes in friction and wear parameters and structural and energy indicators with increasing specific contact load, supporting the use of these criteria to assess their tribological behaviour.

The results revealed ranges of normal friction and wear. Over 8–14 MPa, the ZrO_2–5.3% Y_2O_3 ceramic maintained a stable coefficient of friction of approximately 0.056–0.062, while Fe–Cu exhibited values of approximately 0.09–0.11. Cu–Pb 50/50 exhibited a higher coefficient of friction than Cu–Pb 70/30 over 4–14 MPa.

The material ranking based on energy indicators differed from that based on the coefficient of friction. Fe–Cu exhibited the highest peak specific work of surface degradation and the highest stable level of the thermal energy indicator, whereas the ceramic maintained the lowest coefficient of friction. These differences indicate that the parameters characterise complementary aspects of material behaviour.

Examination of the Fe–Cu friction surface indicated a dynamic balance between the formation and destruction of dissipative secondary structures (DSS) in the normal friction and wear regime. Upon reaching the critical load, this balance shifted towards faster DSS destruction, leading to bulk damage to the surface layer.

Material selection for heavily loaded tribological interfaces should be based on the combined assessment of tribological parameters, structural and energy indicators, and DSS formation and destruction processes. A low coefficient of friction alone is insufficient to establish superior wear resistance.

REFERENCES

[1] Aulin V. Physical basis of processes and states of self-organization in tribotechnical systems. Monograph. V.F. Lysenko Publisher. Kirovograd. 2014. 370 p.

[2] Kostetsky B.I. Structural-energetic adaptability of materials under friction. Friction and Wear 6, 2 (1985) 201–212.

[3] Bernát R., Žarnovský J., Kováč I., Mikuš R., Fries J., Csintalan R. Microanalysis of worn surfaces of selected rotating parts of an internal combustion engine. Materials 15, 1 (2021) 158.

[4] Starczewski L., Szumniak J. Mechanisms of transferring the matter in a friction process in a tribology system: polymeric composite-metal. Surface and Coatings Technology 100 (1998) 33–37.

[5] Al-Quraan T.M., Mikosyanchik O.O., Mnatsakanov R.G., Zaporozhets O.I. Structural-energy characteristics of tribotechnical contact in unsteady operational modes. Modern Mechanical Engineering 6, 3 (2016) 91–97.

[6] Kučera M., Kučera M., Pršan J. Possibilities for classification of tribological processes with regard to energy. Acta Technologica Agriculturae 15, 4 (2012) 89–92.

[7] Kolesnikov V.I. Nonclassical innovative methodology of development of compatibility of metal-polymer tribosystems. Journal of Friction and Wear 36 (2015) 557–558.

[8] Adetunla A., Afolalu S., Jen T.C., Ogundana A. The advances of tribology in materials and energy conservation and engineering innovation. E3S Web of Conferences 391 (2023) 01014.

[9] Dykha A., Padgurskas J., Babak O. Prediction of the life time of cylindrical tribosystems of a vehicle. IOP Conference Series: Materials Science and Engineering 1021, 1 (2021) 012036.

[10] Rodichev A.Y., Novikov A.N., Gorin A.V., Tokmakov N.V. Technological support for the durability of the balancing suspension of the car. IOP Conference Series: Materials Science and Engineering 971, 5 (2020) 052081.

[11] Dykha A., Artiukh V., Sorokatyi R., Kukhar V., Kulakov K. Modeling of wear processes in a cylindrical plain bearing. In: Energy Management of Municipal Transportation Facilities and Transport. Springer International Publishing. Cham. 2019. 542–552.

[12] Ismailov G.M., Tyurin A.E., Gavrilin A.N., Nevinitsyna V.S., Lomovskaya S.A. Study of the identification model of tribological interaction of friction couples. IOP Conference Series: Materials Science and Engineering 919, 2 (2020) 022056.

[13] Vojtov V., Biekirov A., Voitov A. The quality of the tribosystem as a factor of wear resistance. International Journal of Engineering & Technology 7, 4.3 (2018) 25–29.

[14] Aulin V., Lyashuk O., Gupka A., Tson O., Mironov D., Sokol M., Leshchuk R., Yarema I. Tribodiagnosis of the surface damage of tribo-coupling parts materials during machine operation. Procedia Structural Integrity 59 (2024) 428–435.

[15] Hupka A.B. Tribometer for the study of operational materials in the automotive industry. Patent of Ukraine No. 161421. Application No. u202502477. IPC G01N19/02. Published 03.12.2025. Bulletin No. 49/2025